

6G OFDM Communications with High Mobility Transceivers and Scatterers via Angle-Domain Processing and Deep Learning

Mauro Marchese*, Musa Furkan Keskin†, Henk Wymeersch†, Pietro Savazzi*‡

*University of Pavia, Italy, †Chalmers University of Technology, Sweden, ‡CNIT Consorzio Nazionale

Interuniversitario per le Telecomunicazioni, Pavia, Italy

E-mail: mauro.marchese01@universitadipavia.it

Abstract—High-mobility communications, which are crucial for next-generation wireless systems, cause the orthogonal frequency division multiplexing (OFDM) waveform to suffer from strong intercarrier interference (ICI) due to the Doppler effect. In this work, we propose a novel receiver architecture for OFDM that leverages the angular domain to separate multipaths. A block-type pilot is sent to estimate direction-of-arrivals (DoAs), propagation delays, and channel gains of the multipaths. Subsequently, a decision-directed (DD) approach is employed to estimate and iteratively refine the Dopplers. Two different approaches are investigated to provide initial Doppler estimates: an error vector magnitude (EVM)-based method and a deep learning (DL)-based method. Simulation results reveal that the DL-based approach allows for constant bit error rate (BER) performance up to the maximum 6G speed of 1000 km/h.

Index Terms—OFDM, ICI cancellation, parameter estimation, data detection, deep learning.

I. INTRODUCTION

Toward the implementation of next-generation wireless systems, novel use cases are emerging, including high-speed railways (HSR), vehicle-to-everything (V2X), unmanned aerial vehicle (UAV) operations, and autonomous vehicle scenarios. In these 6G high-mobility use cases, speeds of up to 1000 km/h can be encountered [1], [2]. The well-known orthogonal frequency division multiplexing (OFDM) waveform, although suited for combating intersymbol interference (ISI) effects, suffers from intercarrier interference (ICI) caused by the Doppler effect and experiences performance degradation as mobility increases [3]–[5]. More recently, several waveforms have been introduced to overcome these OFDM limitations [6]. Specifically, orthogonal time frequency space (OTFS) modulation was introduced in [4], leveraging communication in the delay-Doppler domain. Typically, in OFDM systems, channel estimation is performed by sending pilot sequences to estimate the channel frequency response (CFR). Conversely, in OTFS systems, channel estimation is usually modeled as a parameter estimation problem due to the sparse nature of the channel in the delay-Doppler domain. Furthermore, channel parameters (channel gains, propagation delays, Doppler

shifts and angles) typically exhibit longer coherence times compared to the CFR [7]. This property is exploited in [7], [8], where channel estimation in OFDM systems is formulated as a parameter estimation problem to leverage the longer coherence time of delay-Doppler coordinates and reduce the number of parameters to be estimated. In [9]–[12], angle-domain separability is exploited to compensate for Doppler shifts separately by transforming the multipath channel into multiple parallel single-Doppler channels. Solutions based on angle-domain processing for both sparse channels [9] and rich scattering environments [10]–[12] have been investigated. However, in these studies, only the Doppler shift induced by the receiver mobility has been considered. Therefore, Doppler estimation is simply reduced to the estimation of the maximum Doppler shift [10]–[12]. The single Doppler shifts affecting each path are then recovered and compensated based on the direction-of-arrival (DoA) [9]–[12]. Moreover, performance investigation across the entire range of 6G speeds has not been done. Thus, the following question remains unanswered: *is it possible to adopt angle-domain based multi-antenna OFDM receivers for 6G high-mobility communications with multiple mobile scatterers?*

In order to answer this question, in this work, a deep learning (DL)-empowered multi-antenna OFDM receiver is developed by relaxing the assumptions made in [9]–[12]. Both parameter-based channel estimation [7], [8] and multipath separation in the angular domain [9] are exploited. The contributions of this work can be summarized as follows:

- **Multi-antenna OFDM receiver with decision-directed (DD)-based multiple Doppler estimation:** A DoA-aided OFDM receiver using a block-type pilot [10] is developed. Multipaths are separated in the angular domain and processed path-wise. Furthermore, a DD approach, leveraging hard decisions as additional pilots, is used to estimate and refine multiple Dopplers by tracking the phase of time-varying channel gains.
- **Enhancement of initial Doppler estimate via DL:** The zero Doppler initialization assumed in the DD approach sets a maximum modulation-dependent speed that the receiver can handle. In order to overcome this limitation, a DL-based approach is introduced to provide accurate initial Doppler estimates.

This work is supported, in part, by the European Union under the Italian National Recovery and Resilience Plan (NRRP) of NextGenerationEU, partnership on “Telecommunications of the Future” (PE00000001 - program “RESTART”) and the Swedish Research Council (Grant 2022-03007 and 2024-04390).

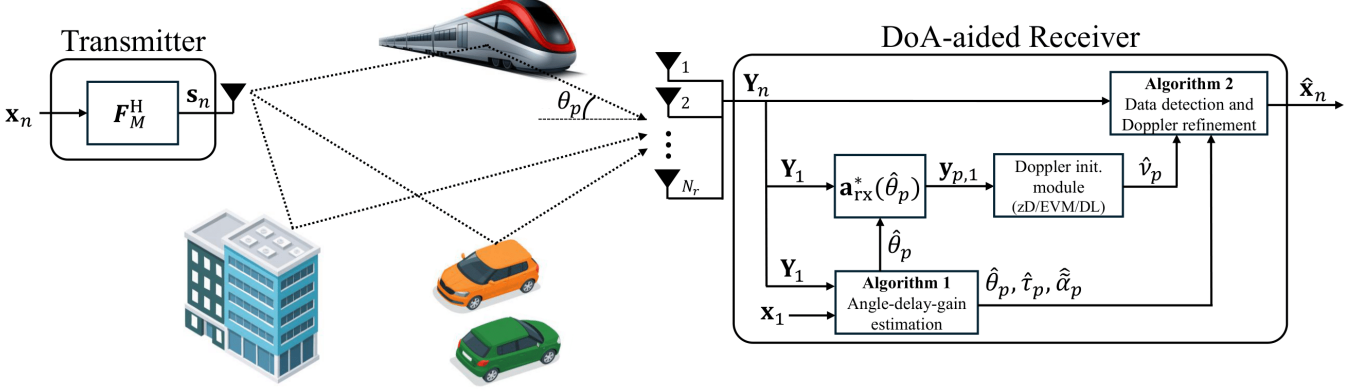


Fig. 1: The OFDM system including a single-antenna transmitter, multiple reflectors (either static or mobile) and the proposed multi-antenna DoA-aided receiver containing a Doppler initialization module for coarse Doppler estimation from the received block-type pilot (zero Doppler, error vector magnitude or deep learning).

- **Mobility-resilience investigation for 6G deployments:**

Simulations are carried out to investigate the robustness of the proposed DoA-aided OFDM receiver against mobility. Results show that the DL-based approach allows performance to be reinforced against high mobility, achieving an almost constant bit error rate (BER) up to the maximum 6G speed of 1000 km/h [1], [2].

II. SYSTEM MODEL

A scenario including a single-antenna transmitter (TX) and a multi-antenna receiver (RX) equipped with a uniform linear array (ULA) with N_r receiving antennas is considered. The system works at carrier frequency f_c . The antenna spacing at the RX is $d = \lambda/2$, where $\lambda = c/f_c$ is the wavelength and c denotes the speed of light.

A. Single-Antenna OFDM Transmitter

The TX sends a block-type pilot to the RX for channel estimation, followed by data frames using OFDM signals. The OFDM symbol is composed of M subcarriers with spacing $\Delta f = 1/T$, where T is the symbol duration. Thus, the signal bandwidth is $B = M\Delta f$. As in classical OFDM transmission, the transmit OFDM symbol is preceded by a cyclic prefix (CP) with duration $T_{CP} > \sigma_\tau$, where σ_τ is the channel delay spread. Hence, the overall symbol duration is $T' = T + T_{CP}$. The delay and Doppler resolutions are $\Delta\tau = 1/B = T/M$ and $\Delta\nu = \Delta f$, respectively. Moreover, the TX sends N OFDM symbols within a geometric coherence time of the channel. Within this time, channel parameters (channel gains, propagation delays, Dopplers, and angles) are assumed to be constant [13]. The TX sends a block-type pilot followed by $N - 1$ OFDM data symbols. The OFDM modulator arranges symbols, taken from alphabet \mathcal{C} , in the frequency domain over the M subcarriers. Hence, the symbol vector $\mathbf{x}_n \in \mathbb{C}^M$ is transmitted during the n -th symbol duration. The information symbols are normalized such that $\mathbb{E}[|\mathbf{x}_n|_m|^2] = 1$. The transmit signal is given as [14]

$$s_n(t) = \sqrt{\frac{P_T}{M}} \sum_{m=0}^{M-1} [\mathbf{x}_n]_m e^{j2\pi m \Delta f t} \Pi\left(\frac{t - nT'}{T'}\right), \quad (1)$$

where $\Pi(t)$ is a rectangular pulse that takes the value 1 for $t \in [0, 1]$ and 0 otherwise, and P_T is the average transmit power.

B. Observation Model at the Multi-Antenna Receiver

Let's consider a transmission over a wireless channel made of P propagation paths each with delay τ_p , Doppler shift ν_p , channel gain α_p and DoA θ_p . The channel response of the single-input multiple-output (SIMO) channel is given as

$$\mathbf{h}(t, \tau) = \sum_{p=1}^P \alpha_p e^{j2\pi\nu_p t} \delta(\tau - \tau_p) \mathbf{a}_{rx}(\theta_p) \in \mathbb{C}^{N_r}, \quad (2)$$

where $\mathbf{a}_{rx}(\theta) = [1 \quad e^{j\frac{2\pi}{\lambda}d\sin(\theta)} \quad \dots \quad e^{j\frac{2\pi}{\lambda}d(N_r-1)\sin(\theta)}]^T$ is the steering vector of the ULA at the RX. During the n -th symbol time, the received signal at the N_r antennas is obtained as

$$\begin{aligned} \mathbf{y}_n^{CP}(t) &= \int \mathbf{h}(t, \tau) s_n^{CP}(t - \tau) d\tau + \mathbf{n}(t) \\ &= \sum_{p=1}^P \alpha_p s_n^{CP}(t - \tau_p) e^{j2\pi\nu_p t} \mathbf{a}_{rx}(\theta_p) + \mathbf{n}(t) \in \mathbb{C}^{N_r}, \end{aligned} \quad (3)$$

where $\mathbf{n}(t)$ is additive white gaussian noise (AWGN) with a one-sided power spectral density (PSD) N_0 , and $s_n^{CP}(t)$ denotes the transmit signal with the CP. After sampling at the symbol rate and CP removal, the received time-spatial observations $\mathbf{Y}_n \in \mathbb{C}^{M \times N_r}$ during the n -th symbol time are obtained as [14], [15]

$$\begin{aligned} \mathbf{Y}_n &= \sum_{p=1}^P \alpha_p e^{j2\pi\nu_p t_n} \mathbf{C}(\nu_p) \mathbf{F}_M^H \mathbf{B}(\tau_p) \mathbf{F}_M \mathbf{s}_n \mathbf{a}_{rx}^\top(\theta_p) + \mathbf{N} \\ &= \sqrt{P_T} \sum_{p=1}^P \tilde{\alpha}_{p,n} [\mathbf{F}_M^H (\mathbf{x}_n \odot \mathbf{b}(\tau_p)) \odot \mathbf{c}(\nu_p)] \mathbf{a}_{rx}^\top(\theta_p) + \mathbf{N}, \end{aligned} \quad (4)$$

where $\mathbf{s}_n = \sqrt{P_T} \mathbf{F}_M^H \mathbf{x}_n \in \mathbb{C}^M$ is the transmit signal vector where $[\mathbf{F}_M]_{m,q} = \frac{1}{\sqrt{M}} e^{-j2\pi \frac{mq}{M}}$ denotes the M -point discrete Fourier transform (DFT) matrix. Moreover, $\mathbb{E}[|\mathbf{s}_n|^2] = M P_T$; $\mathbf{N} \in \mathbb{C}^{M \times N_r}$ is the AWGN matrix and $\text{vec}(\mathbf{N}) \sim \mathcal{CN}(\mathbf{0}, \sigma^2 \mathbf{I}_{MN_r})$. Noise variance is given as $\sigma^2 = N_0 B$ and $\mathbb{E}[|\mathbf{N}|^2] = M N_r \sigma^2$; $\mathbf{B}(\tau) = \text{diag}(\mathbf{b}(\tau))$, where $\mathbf{b}(\tau) = [e^{-j2\pi q\tau \Delta f}]_{q=0}^{M-1}$; $\mathbf{C}(\nu) = \text{diag}(\mathbf{c}(\nu))$, where

$\mathbf{c}(\nu) = [e^{j2\pi q\nu\Delta\tau}]_{q=0}^{M-1}$ captures fast-time effects caused by Doppler (i.e. ICI); $\tilde{\alpha}_{p,n} = \alpha_p e^{j2\pi\nu_p t_n}$ is the Doppler-induced time varying channel gain that captures slow-time variations where $t_n = nT_{\text{CP}} + (n-1)T$ is the time at which the transmission of the n -th OFDM symbol starts. The signal-to-noise ratio (SNR) is obtained as $\text{SNR} = \|\alpha\|^2 P_T / (N_0 B)$ where $\alpha = [\alpha_1, \alpha_2, \dots, \alpha_P]^\top$ is the channel gains vector.

III. PROPOSED DOA-AIDED OFDM RECEIVER

In this section the architecture of the proposed DoA-aided receiver is presented. First, multipath separation in the angle-domain is discussed; afterwards, delay compensation, ICI cancellation and channel parameter estimation with DD Doppler estimation are presented.

A. Path Separation via Angle-domain Matched Filter

Assuming that the RX is equipped with a large ULA, different directions are approximately orthogonal [10]; i.e. $\mathbf{a}_{\text{rx}}^\top(\theta_1)\mathbf{a}_{\text{rx}}^*(\theta_2) \approx 0$ if $\theta_1 \neq \theta_2$. Consequently, a matched filter (MF) can be applied to separate multipaths by computing

$$\begin{aligned} \mathbf{y}_{p,n} &= \frac{\mathbf{Y}_n \mathbf{a}_{\text{rx}}^*(\theta_p)}{N_r} = \sqrt{P_T} \tilde{\alpha}_{p,n} [\mathbf{F}_M^\text{H} (\mathbf{x}_n \odot \mathbf{b}(\tau_p)) \odot \mathbf{c}(\nu_p)] + \\ &\quad \underbrace{\sqrt{P_T} \sum_{\substack{i=1 \\ i \neq p}}^P \tilde{\alpha}_{i,n} \mathbf{a}_{\text{rx}}^\top(\theta_i) \mathbf{a}_{\text{rx}}^*(\theta_p) [\mathbf{F}_M^\text{H} (\mathbf{x}_n \odot \mathbf{b}(\tau_i)) \odot \mathbf{c}(\nu_i)] + \mathbf{n}_p}_{\text{IPI}} \\ &\approx \sqrt{P_T} \tilde{\alpha}_{p,n} [\mathbf{F}_M^\text{H} (\mathbf{x}_n \odot \mathbf{b}(\tau_p)) \odot \mathbf{c}(\nu_p)] + \mathbf{n}_p \in \mathbb{C}^M, \end{aligned} \quad (5)$$

where the second term is known as interpath interference (IPI) and approaches zero as $N_r \rightarrow \infty$. Moreover, $\mathbf{n}_p = \mathbf{N} \mathbf{a}_{\text{rx}}^*(\theta_p) / N_r$ is noise with variance $\sigma_p^2 = \mathbb{E}[\|\mathbf{n}_p\|^2] / M$. Since $\mathbb{E}[\mathbf{N}^\text{H} \mathbf{N}] = M\sigma^2 \mathbf{I}_{N_r}$ and $\|\mathbf{a}_{\text{rx}}(\theta_p)\|^2 = N_r$, the noise variance after beamforming is $\sigma_p^2 = \sigma^2 / N_r$.

B. Data Detection: Delay/ICI Compensation

In this section, data detection is discussed assuming knowledge of channel parameters. The architecture of the DoA-aided receiver performing both estimation and data detection is discussed in the next section.

1) *ICI Cancellation via Time-Domain Single-tap MF*: Given the impaired observation $\mathbf{y}_{p,n}$, the effect of the Doppler shift ν_p can be compensated for by computing¹

$$\mathbf{y}_{p,n}^{\text{ICI}} = \mathbf{y}_{p,n} \odot \mathbf{c}^*(\hat{\nu}_p) \approx \sqrt{P_T} \tilde{\alpha}_{p,n} \mathbf{F}_M^\text{H} (\mathbf{x}_n \odot \mathbf{b}(\tau_p)) + \mathbf{n}_p. \quad (6)$$

2) *Delay compensation via Frequency-Domain Single-tap MF*: Given the ICI-compensated observation $\mathbf{y}_{p,n}^{\text{ICI}}$, the effect of the propagation delay τ_p can be compensated for by computing the frequency domain ICI-compensated symbols

$$\mathbf{x}_{p,n}^{\text{ICI}} = \mathbf{F}_M \mathbf{y}_{p,n}^{\text{ICI}} \approx \sqrt{P_T} \tilde{\alpha}_{p,n} (\mathbf{x}_n \odot \mathbf{b}(\tau_p)) + \mathbf{n}_p, \quad (7)$$

and applying a single-tap MF as

$$\hat{\mathbf{x}}_{p,n} = \mathbf{x}_{p,n}^{\text{ICI}} \odot \mathbf{b}^*(\hat{\tau}_p) \approx \sqrt{P_T} \tilde{\alpha}_{p,n} \mathbf{x}_n + \mathbf{n}_p. \quad (8)$$

¹Considering a single-path impaired signal, ICI can be easily compensated for by using $\mathbf{c}(\nu) \odot \mathbf{c}^*(\nu) = \mathbf{1}$. The same holds also for the delay shift.

Algorithm 1: Proposed angle-delay-gain estimation

Input: $\mathbf{Y}_1, \mathbf{x}_1$

Path detection and DoA estimation:

Run CFAR to $\mathcal{P}(\theta) = \|\mathbf{Y}_1 \mathbf{a}_{\text{rx}}^*(\theta)\|^2$ and obtain estimated DoAs $\{\hat{\theta}_p\}_{p=1}^{\hat{P}}$

Delay-gain estimation:

for $p = 1$ **to** \hat{P} **do**

$$\left| \begin{array}{l} \mathbf{y}_{p,1} = \frac{\mathbf{Y}_1 \mathbf{a}_{\text{rx}}^*(\hat{\theta}_p)}{N_r} \\ \hat{\tau}_p = \arg \max_{\tau} |\tilde{\mathbf{b}}^H(\tau) \mathbf{y}_{p,1}| \\ \hat{\tilde{\alpha}}_{p,1} = \frac{\tilde{\mathbf{b}}(\hat{\tau}_p)^H \mathbf{y}_{p,1}}{M \sqrt{P_T}} \end{array} \right.$$

Output: $\{\hat{\theta}_p, \hat{\tau}_p, \hat{\tilde{\alpha}}_{p,1}\}_{p=1}^{\hat{P}}$

3) *Maximum ratio combining*: Following the previous steps, P estimates of the information symbols are obtained ($\hat{\mathbf{x}}_{p,n}$). In order to maximize SNR, maximum ratio combining (MRC) can be used to obtain the estimated symbols as $\hat{\mathbf{x}}_n = \sum_{p=1}^P \hat{\tilde{\alpha}}_{p,n}^* \hat{\mathbf{x}}_{p,n} \approx \sqrt{P_T} \|\alpha_n\|^2 \mathbf{x}_n + \sum_{p=1}^P \hat{\tilde{\alpha}}_{p,n}^* \mathbf{n}_p$, where $\alpha_n = [\hat{\alpha}_{1,n}, \hat{\alpha}_{2,n}, \dots, \hat{\alpha}_{P,n}]^\top$. In conclusion, assuming accurate parameter estimation and negligible IPI due to large number of antenna elements, the proposed DoA-aided receiver transforms the doubly-dispersive channel into an equivalent channel affected by additive noise.

C. Channel Parameter Estimation

Given the OFDM system model in Section II, the following estimation algorithm is proposed. A more detailed description is provided in Algorithm 1 and Algorithm 2.

1) *Angle Estimation*: The estimation of the DoA for each path is carried out by computing the received power as a function of the direction θ as $\mathcal{P}(\theta) = \|\mathbf{Y}_1 \mathbf{a}_{\text{rx}}^*(\theta)\|^2$. Thus, the DoAs can be estimated by searching for peaks in the angular spectrum by running a constant false alarm rate (CFAR) detector to set an adaptive threshold.

2) *Angle-domain MF*: A MF is applied to separate the detected multipaths, as shown in (5). Therefore, the received block-type pilot is given as $\mathbf{y}_{p,1} = \sqrt{P_T} \tilde{\alpha}_{p,1} \tilde{\mathbf{b}}(\tau_p) \odot \mathbf{c}(\nu_p) + \mathbf{n}_p$, where $\tilde{\mathbf{b}}(\tau) = \mathbf{F}_M^\text{H} (\mathbf{x}_1 \odot \mathbf{b}(\tau))$ is the time-domain delay term.

3) *Delay Estimation*: If the coherence time² $(\Delta t)_c$ becomes comparable with T' , the Doppler-induced ICI can be neglected to perform delay estimation. This approximation is equivalent to considering a constant channel within an OFDM symbol transmission, and therefore, there is no ICI [7]. However, the Doppler must be estimated since it makes the channel response change over time, and ICI should be compensated to avoid performance degradation in data detection. Assuming that this condition holds due to poor Doppler resolution, the MF output can be approximated by $\mathbf{y}_{p,1} \approx \sqrt{P_T} \tilde{\alpha}_{p,1} \tilde{\mathbf{b}}(\tau_p) + \mathbf{n}_p$. Finally, the delay can be estimated as follows: $\hat{\tau}_p = \arg \max_{\tau} |\tilde{\mathbf{b}}^H(\tau) \mathbf{y}_{p,1}|$.

4) *Gain Estimation*: Once a delay-angle pair is obtained, the estimation of the channel gain associated with the p -th path can be done using the least squares (LS) estimator as $\hat{\tilde{\alpha}}_{p,1} = (\tilde{\mathbf{b}}(\hat{\tau}_p)^H \mathbf{y}_{p,1}) / (M \sqrt{P_T})$.

²The coherence time is given as $(\Delta t)_c \approx \frac{1}{\sigma_\nu}$, where $\sigma_\nu = \frac{f_c}{c} v_{\text{max}}$ is the Doppler spread and v_{max} is the maximum speed.

Algorithm 2: Proposed DoA-aided receiver

Input: $\mathbf{Y}_n, \mathbf{x}_1, K, \{\hat{\theta}_p, \hat{\tau}_p, \hat{\alpha}_{p,1}\}_{p=1}^{\hat{P}}$ obtained using Algorithm 1

Initialize: $\hat{\nu}_p = 0$ (zero-Doppler)

Joint data detection and Doppler estimation:

for $n = 2$ **to** $N - K + 1$ **do**

if $n < N - K + 1$ **then**

for $k = 1$ **to** K **do**

for $p = 1$ **to** \hat{P} **do**

$\mathbf{y}_{p,n+k-1} = \frac{\mathbf{Y}_{n+k-1} \mathbf{a}_{\text{tx}}^*(\hat{\theta}_p)}{N_r}$

$\mathbf{y}_{p,n+k-1}^{\text{ICI}} = \mathbf{y}_{p,n+k-1} \odot \mathbf{c}^*(\hat{\nu}_p)$

$\hat{\mathbf{x}}_{p,n+k-1} = \mathbf{F}_M \mathbf{y}_{p,n+k-1}^{\text{ICI}} \odot \mathbf{b}^*(\hat{\tau}_p)$

$\hat{\alpha}_{p,n+k-1} = \hat{\alpha}_{p,n+k-2} e^{j2\pi\hat{\nu}_p T'}$

$\hat{\mathbf{x}}_{n+k-1} = \sum_{p=1}^{\hat{P}} \hat{\alpha}_{p,n+k-1}^* \hat{\mathbf{x}}_{p,n+k-1}$

$\hat{\mathbf{x}}_{n+k-1}^\dagger = \mathcal{C}(\hat{\mathbf{x}}_{n+k-1})$

for $p = 1$ **to** \hat{P} **do**

$\hat{\alpha}_{p,n+k-1} = \frac{[\mathbf{F}_M^H (\hat{\mathbf{x}}_{n+k-1}^\dagger \odot \mathbf{b}(\hat{\tau}_p)) \odot \mathbf{c}(\hat{\nu}_p)]^H \mathbf{y}_{p,n+k-1}}{M \sqrt{P_T}}$

$\hat{\nu}_p = \frac{\angle \hat{\alpha}_{p,n+K-1} \hat{\alpha}_{p,n}^*}{2\pi(K-1)T'}$

for $p = 1$ **to** \hat{P} **do**

$\hat{\mathbf{x}}_{p,n} = \mathbf{F}_M (\mathbf{y}_{p,n} \odot \mathbf{c}^*(\hat{\nu}_p)) \odot \mathbf{b}^*(\hat{\tau}_p)$

$\hat{\mathbf{x}}_n = \sum_{p=1}^{\hat{P}} \hat{\alpha}_{p,n}^* \hat{\mathbf{x}}_{p,n}$

$\hat{\mathbf{x}}_n^\dagger = \mathcal{C}(\hat{\mathbf{x}}_n)$

else

for $k = 1$ **to** K **do**

for $p = 1$ **to** \hat{P} **do**

$\mathbf{y}_{p,n+k-1} = \frac{\mathbf{Y}_{n+k-1} \mathbf{a}_{\text{tx}}^*(\hat{\theta}_p)}{N_r}$

$\mathbf{y}_{p,n+k-1}^{\text{ICI}} = \mathbf{y}_{p,n+k-1} \odot \mathbf{c}^*(\hat{\nu}_p)$

$\hat{\mathbf{x}}_{p,n+k-1} = \mathbf{F}_M \mathbf{y}_{p,n+k-1}^{\text{ICI}} \odot \mathbf{b}^*(\hat{\tau}_p)$

$\hat{\alpha}_{p,n+k-1} = \hat{\alpha}_{p,n-1} e^{j2\pi\hat{\nu}_p k T'}$

$\hat{\mathbf{x}}_{n+k-1} = \sum_{p=1}^{\hat{P}} \hat{\alpha}_{p,n+k-1}^* \hat{\mathbf{x}}_{p,n+k-1}$

$\hat{\mathbf{x}}_{n+k-1}^\dagger = \mathcal{C}(\hat{\mathbf{x}}_{n+k-1})$

Output: $\hat{\mathbf{x}}_n^\dagger$

5) *Decision-Directed Doppler Estimation via Gain Tracking:* A DD approach on the incoming OFDM data symbols is used to obtain an estimate of the Doppler by increasing the observation time. In particular, a sliding window of length $2 < K < N - 1$ ³ is considered to estimate Dopplers. A slicer is adopted to obtain hard decisions (denoted $\hat{\mathbf{x}}_n^\dagger = \mathcal{C}(\hat{\mathbf{x}}_n)$, where $\mathcal{C}(\cdot)$ is the hard decision according to alphabet \mathcal{C}), and decoded data are used as additional pilots to estimate time-varying channel gains through LS. Once channel gains are obtained, the Doppler can be estimated by noting that $\phi_p = \angle \hat{\alpha}_{p,n+K-1} \hat{\alpha}_{p,n}^* \approx 2\pi\nu_p(t_{n+K-1} - t_n) = 2\pi\nu_p(K-1)T'$. Thus, $\hat{\nu}_p = \phi_p/(2\pi(K-1)T')$.

³The parameter K should be selected to avoid wrapping issues. In particular, given the channel Doppler spread σ_ν , K should satisfy $2\pi\sigma_\nu(K-1)T' < \pi$. Equivalently, $K < 1 + \frac{1}{2\sigma_\nu T'}$.

D. Enhancing Initial Doppler Estimate

Due to the zero Doppler (zD) initialization in Algorithm 2, the performance of the proposed approach is limited up to a maximum Doppler of $\nu_{\max} = \frac{1}{8T'}$ ⁴ for 4-QAM, primarily because of the rapidly varying phase of the channel gain $\hat{\alpha}_{p,n}$. Consequently, the hard decisions $\hat{\mathbf{x}}_n^\dagger$ are subject to decision errors that stem solely from the uncompensated Doppler-induced phase rotation resulting from the zD initialization assumed in Section III-C. In order to enhance performance at higher speeds without increasing Δf (and thereby deteriorating spectral efficiency), an initial guess of the Doppler must be provided. This prevents error propagation by enabling the RX to track rapid phase rotations in subsequent OFDM symbols. The following approaches are investigated:

1) *EVM Minimization:* The Doppler effect causes ICI in the signal within each branch, which, in turn, increases the error vector magnitude (EVM). Therefore, an initial guess of the Doppler can be obtained by searching for a coarse Doppler shift that minimizes the EVM. Thus $\hat{\nu}_p = \arg \min_\nu \text{EVM}_p(\nu)$, where

$$\text{EVM}_p(\nu) = \frac{1}{M} \left\| \frac{\mathbf{F}_M [\mathbf{y}_{p,1} \odot \mathbf{c}^*(\nu)] \odot \mathbf{b}^*(\hat{\tau}_p)}{\hat{\alpha}_{p,1} \sqrt{P_T}} - \mathbf{x}_1 \right\|^2. \quad (9)$$

2) *DL-based Approach:* A DL architecture, which performs a regression task, is used to predict the Doppler shift from the received block-type pilot. In particular, a feedforward neural network (FNN) receives $\mathbf{y}_{p,1}/(\hat{\alpha}_{p,1} \sqrt{P_T})$ as input and provides a coarse estimate of the Doppler affecting the p -th path ($\hat{\nu}$) as output. The objective function for the optimization problem is the mean squared error (MSE) $\mathcal{L}(\hat{\nu}, \nu) = |\hat{\nu} - \nu|^2$.

E. Resource Allocation and Utilization

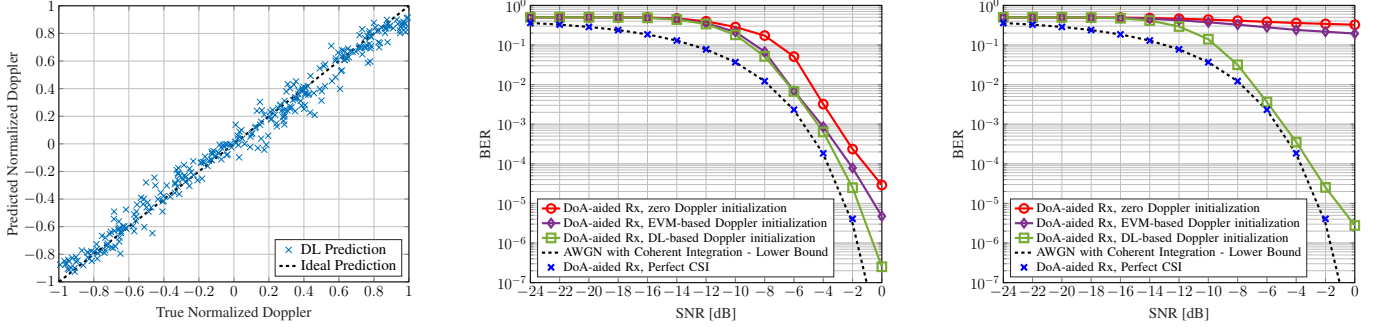
1) *Pilot Overhead:* A single OFDM block is used for estimating channel parameters, thus the effective pilot overhead is $1/N$. Assuming a geometric coherence time of 10 ms⁵, an OFDM symbol duration of $T = 33.3 \mu\text{s}$ with a subcarrier spacing of $\Delta f = 30 \text{ kHz}$ and a CP duration of $5 \mu\text{s}$, the minimum overhead for a continuous transmission is about 0.38%. However, for a short frame duration of 1 ms, the overhead is less than 4%.

2) *Complexity:* The complexity of the proposed receiver is dominated by the joint Doppler estimation and data detection procedure with a sliding buffer, thus the complexity is $\mathcal{O}(NKPMN_r) + \mathcal{O}(NKPM \log(M))$. The EVM- and DL-based Doppler initialization modules have complexities of $\mathcal{O}(M \log(M))$ and $\mathcal{O}(M^2)$, respectively.

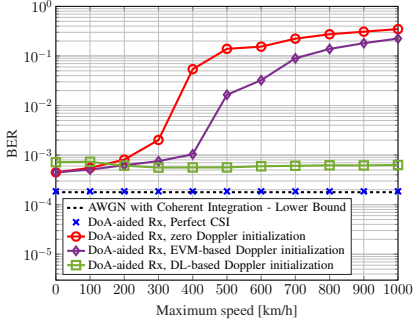
3) *Decoding Latency:* The sliding buffer used for Doppler refinement in Algorithm 2 introduces a latency in decoding OFDM symbols of KT' .

⁴The maximum Doppler supported by the proposed approach can be computed by noting that the maximum large-scale Doppler-induced phase rotation can be at most $\pi/4$ when using 4-quadrature amplitude modulation (QAM) signaling. Therefore, $2\pi\nu_{\max}T' < \frac{\pi}{4}$.

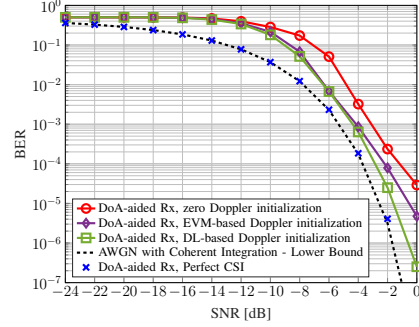
⁵In 6G high-mobility scenarios, the geometric coherence time can be in the order of tens of milliseconds [13], depending on the velocity of mobile scatterers.



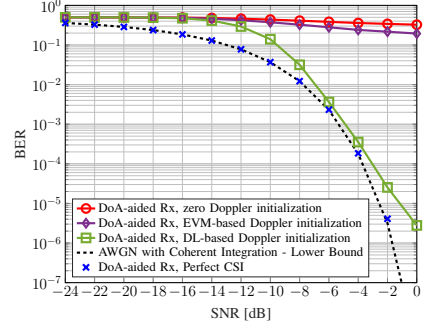
(a) DL-based Doppler predictions are shown against true values. Both are normalized with respect to the maximum Doppler shift used during training.



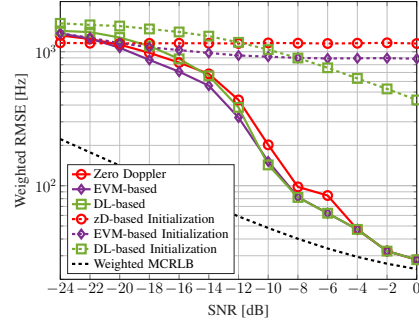
(d) The BER is shown against maximum UE velocity with a fixed SNR = -4 dB. The proposed DoA-aided approach in doubly-dispersive channel is compared against AWGN with coherent integration.



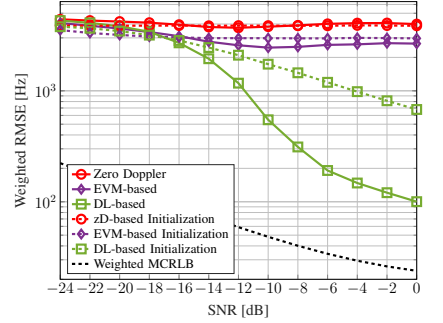
(b) The BER is shown against SNR for a maximum UE speed of 300 km/h. The proposed DoA-aided approach in doubly-dispersive channel is compared against AWGN with coherent integration.



(c) The BER is shown against SNR for a maximum UE speed of 1000 km/h. The proposed DoA-aided approach in doubly-dispersive channel is compared against AWGN with coherent integration.



(e) The RMSE is shown against SNR for the different initialization approaches and maximum UE speed of 300 km/h. The MCRBL is shown as a theoretical limit for estimation performance.



(f) The RMSE is shown against SNR for the different initialization approaches and maximum UE speed of 1000 km/h. The MCRBL is shown as a theoretical limit for estimation performance.

Fig. 2: Simulation results for varying Doppler, SNR, and UE speed.

TABLE I: Simulation parameters.

General	
Carrier frequency, f_c	5.9 GHz
Number of antennas, N_r	32
Number of subcarriers, M	128
Number of OFDM symbols, N	32
Subcarrier spacing, Δf	30 kHz
CP duration, T_{CP}	5 μ s
Modulation	4-QAM
Sliding window dimension, K	$\min(\lfloor 1 + \frac{1}{2\sigma_\nu T'} \rfloor, N/2)$
Wireless channel	
Number of multipaths, P	4
Direction of arrivals, θ_p	$[10^\circ, 50^\circ, -30^\circ, 20^\circ]$
Propagation delays, τ_p	$[0, 0.9, 2.4, 3]$ μ s
Average power per path, \mathcal{P}_p	$[0, -1, -5, -7]$ dB
Doppler shifts, ν_p	$\nu_p = f_c \frac{v_{\max}}{c} \cos(\theta_p)$ $\theta_p \sim \mathcal{U}[0, 2\pi]$

IV. SIMULATION RESULTS

Numerical simulations are performed to validate the proposed approach. Table I summarizes the simulation parameters. The FNN is composed of four layers with dimensions $\{M, M, \frac{M}{2}, \frac{M}{2}\}$. The layers are fully connected, and each layer employs a rectified linear unit (ReLU) as the activation function, except for the last layer, which adopts a linear activation in order to provide real numbers as output. The FNN is trained with $5 \cdot 10^5$ pilot samples (80% training, 20% validation) affected by random delay, Doppler, and SNR. In particular, the delay and Doppler are uniformly distributed as $\tau \sim \mathcal{U}[0, 5]$ μ s and $\nu \sim \mathcal{U}[-5, 5]$ kHz, and $\text{SNR} \sim \mathcal{U}[12, 18]$ dB. The pilot samples are synthetically generated using $\mathbf{F}_N^H(\mathbf{x}_1 \odot \mathbf{b}(\tau)) \odot \mathbf{c}(\nu) + \mathbf{w}$, where $\mathbf{w} \sim \mathcal{CN}(\mathbf{0}, \mathbf{I}/\text{SNR})$. Figure 2a shows the predicted Dopplers against true values,

and it can be noted that the DL architecture is actually capable of estimating the Doppler from the received block-type pilot.

Figure 2b and Figure 2c show the BER performance against SNR for maximum speeds of 300 km/h and 1000 km/h, respectively. It can be noted that, in both scenarios, the proposed DoA-aided receiver with perfect channel state information (CSI) achieves the same performance as OFDM over an AWGN channel with coherent integration. For a 4-QAM, this lower bound can be approximated as $Q(\sqrt{N_r \text{SNR}})$, where $Q(\cdot)$ denotes the Gaussian Q-function. Moreover, when considering imperfect CSI, the DL-based Doppler initialization achieves BER performance close to the AWGN lower bound at sufficient SNR values. Conversely, the zD- and EVM-based initialization schemes underperform the DL-based approach and, in the case of a maximum speed of 1000 km/h, they fail completely. Figure 2d shows the BER performance against the maximum speed. It can be noted that, unlike the cases of zD- and EVM-based initialization, which start failing at speeds higher than 300 km/h and 400 km/h respectively, the DL-based approach achieves an almost constant BER up to the maximum 6G speed of 1000 km/h. Accordingly, Figure 2e and Figure 2f show the Doppler weighted root mean squared error (RMSE), defined as

$$\text{Weighted RMSE} = \sqrt{\mathbb{E} \left[\frac{\sum_{p=1}^P |\alpha_p|^2 (\nu_p - \hat{\nu}_p)^2}{\|\alpha\|^2} \right]}, \quad (10)$$

against SNR for maximum speeds of 300 km/h and 1000 km/h, respectively. It can be noted that the DL-based initialization effectively provides more accurate coarse estimates than EVM-

based initialization. Moreover, the proposed Doppler estimation via gain tracking achieves performance sufficiently close to the modified Cramér-Rao Lower Bound (MCRLB) for all the initialization approaches when the maximum speed is 300 km/h. Conversely, in the case of a maximum speed of 1000 km/h, only the DL-based approach reaches low RMSE.

V. CONCLUSIONS AND FUTURE WORKS

In this work, a multi-antenna RX, empowered by DL, for SIMO-OFDM is developed. A mobility-resilience numerical analysis is carried out to validate the proposed scheme. Simulation results reveal that the proposed DL-based approach achieves almost constant BER up to a maximum speed of 1000 km/h with low pilot overhead (less than 4%) and low complexity inherited from simple operations (single-tap delay compensation and ICI cancellation, DFT, and gain tracking) at the cost of introducing a decoding latency due to the sliding buffer, making DoA-aided receivers suitable for 6G high-mobility communications. Future research will further investigate the impact of higher-order QAM constellations and the effect of multiple paths with the same angle, which results in higher IPI.

APPENDIX

MODIFIED CRAMÉR-RAO LOWER BOUND FOR DOPPLER

The weighted MCRLB for the Doppler shift is computed as follows. Assuming small IPI due to large ULA at the RX, the conditional Fisher information (CFI) at the n -th OFDM symbol is approximated using the Slepian-Bangs formula [16] as

$$\mathcal{I}_{p,n}(\nu_p|\alpha_p, \mathbf{x}_n) \approx \frac{2}{\sigma^2 + \mathcal{P}_{\text{IPI}}^{(p)}} \left\| \frac{\partial \boldsymbol{\mu}_p}{\partial \nu_p} \right\|^2, \quad (11)$$

where $\boldsymbol{\mu}_p = \sqrt{P_T} \alpha_p e^{j2\pi\nu_p t_n} [\mathbf{F}_M^H(\mathbf{x}_n \odot \mathbf{b}(\tau_p)) \odot \mathbf{c}(\nu_p)]$ from (5) and $\mathcal{P}_{\text{IPI}}^{(p)} = P_T |\alpha_p|^2 \sum_{i=1}^P (1 - \delta_{ip}) |\mathbf{a}^\top(\theta_p) \mathbf{a}^*(\theta_i)|^2$. Therefore, the derivative is

$$\left[\frac{\partial \boldsymbol{\mu}_p}{\partial \nu_p} \right]_q = \frac{j2\pi(t_n + q\Delta\tau)\sqrt{P_T}\alpha_p}{e^{-j2\pi\nu_p(t_n + q\Delta\tau)}} \left[\mathbf{F}_M^H(\mathbf{x}_n \odot \mathbf{b}(\tau_p)) \right]_q. \quad (12)$$

Thus, the CFI becomes

$$\mathcal{I}_{p,n}(\nu_p|\alpha_p, \mathbf{x}_n) \approx \frac{8\pi^2 |\alpha_p|^2 P_T}{\sigma^2 + \mathcal{P}_{\text{IPI}}^{(p)}} \sum_{q=0}^{M-1} (t_n + q\Delta\tau)^2 \left| \left[\mathbf{F}_M^H(\mathbf{x}_n \odot \mathbf{b}(\tau_p)) \right]_q \right|^2. \quad (13)$$

In particular, for $n = 1$ (deterministic pilot)

$$\mathcal{I}_{p,1}(\nu_p|\alpha_p) \approx \frac{8\pi^2 |\alpha_p|^2 P_T}{\sigma^2 + \mathcal{P}_{\text{IPI}}^{(p)}} \sum_{q=0}^{M-1} (T_{\text{CP}} + q\Delta\tau)^2 \left| \left[\tilde{\mathbf{b}}(\tau_p) \right]_q \right|^2. \quad (14)$$

The aggregated averaged information comprising the N received observations is given as

$$\begin{aligned} \mathcal{I}_p(\nu_p) &= \mathbb{E}_\alpha [\mathcal{I}_{p,1}(\nu_p|\alpha_p)] + \sum_{n=2}^N \mathbb{E}_{\alpha, \mathbf{x}} [\mathcal{I}_{p,n}(\nu_p|\alpha_p, \mathbf{x}_n)] \approx \\ &\frac{8\pi^2 \mathcal{P}_p P_T}{\sigma^2 + \mathcal{P}_{\text{IPI}}^{(p)}} \left(\sum_{q=0}^{M-1} (T_{\text{CP}} + q\Delta\tau)^2 \left| \left[\tilde{\mathbf{b}}(\tau_p) \right]_q \right|^2 + \|\boldsymbol{\Theta}\|^2 \right), \end{aligned} \quad (15)$$

where $\mathcal{P}_p = \mathbb{E}[|\alpha_p|^2]$ is the average power of the p -th path and $\boldsymbol{\Theta} \in \mathbb{R}^{(N-1)M}$ where $[\boldsymbol{\Theta}]_i = t_n + q\Delta\tau$ with $i = M(n-2) + q$ where $n = 2, \dots, N$ and $q = 0, \dots, M-1$. The MCRLB for the p -th path is then obtained as $\text{MCRLB}_p = \mathcal{I}_p^{-1}(\nu_p)$. Hence, the global weighted bound is

$$\text{Weighted MCRLB} = \frac{\sum_{p=1}^P \mathcal{P}_p \text{MCRLB}_p}{\sum_{p=1}^P \mathcal{P}_p}. \quad (16)$$

REFERENCES

- [1] M. Giordani, M. Polese, M. Mezzavilla, S. Rangan, and M. Zorzi, "Toward 6G Networks: Use Cases and Technologies," *IEEE Communications Magazine*, vol. 58, no. 3, pp. 55–61, 2020.
- [2] H. Tataria, M. Shafi, A. F. Molisch, M. Dohler, H. Sjöland, and F. Tufvesson, "6G Wireless Systems: Vision, Requirements, Challenges, Insights, and Opportunities," *Proceedings of the IEEE*, vol. 109, no. 7, pp. 1166–1199, 2021.
- [3] T. Wang, J. Proakis, E. Masry, and J. Zeidler, "Performance degradation of OFDM systems due to Doppler spreading," *IEEE Transactions on Wireless Communications*, vol. 5, no. 6, pp. 1422–1432, 2006.
- [4] R. Hadani, S. Rakib, M. Tsatsanis, A. Monk, A. J. Goldsmith, A. F. Molisch, and R. Calderbank, "Orthogonal Time Frequency Space Modulation," in *2017 IEEE Wireless Communications and Networking Conference (WCNC)*, 2017, pp. 1–6.
- [5] Y. Mostofi and D. Cox, "ICI mitigation for pilot-aided OFDM mobile systems," *IEEE Transactions on Wireless Communications*, vol. 4, no. 2, pp. 765–774, 2005.
- [6] Y. Zhou, H. Yin, J. Xiong, S. Song, J. Zhu, J. Du, H. Chen, and Y. Tang, "Overview and Performance Analysis of Various Waveforms in High Mobility Scenarios," in *2024 7th International Conference on Communication Engineering and Technology (ICCET)*, 2024, pp. 35–40.
- [7] H. P. H. Shaw, J. Yuan, and M. Rowshan, "Delay-Doppler Channel Estimation by Leveraging the Ambiguity Function in OFDM Systems," in *2023 IEEE International Conference on Communications Workshops (ICC Workshops)*, 2023, pp. 307–313.
- [8] D. Han, Y. Liu, J. Ni, and et al., "Parameter Based Channel Estimation for OFDM Systems Over Time-Varying Channels," *Wireless Personal Communications*, vol. 83, pp. 703–720, 2015.
- [9] Y. Zhang, Q. Yin, P. Mu, and L. Bai, "Multiple Doppler shifts compensation and ICI elimination by beamforming in high-mobility OFDM systems," in *2011 6th International ICST Conference on Communications and Networking in China (CHINACOM)*, 2011, pp. 170–175.
- [10] Y. Ge, W. Zhang, F. Gao, and H. Minn, "Angle-Domain Approach for Parameter Estimation in High-Mobility OFDM With Fully/Partly Calibrated Massive ULA," *IEEE Transactions on Wireless Communications*, vol. 18, no. 1, pp. 591–607, 2019.
- [11] Y. Feng, Z. Zhu, W. Lu, N. Zhao, and A. Nallanathan, "Non-Data-Aided Joint Multi-DFO Estimation for High-Mobility OFDM Communication Systems," *IEEE Transactions on Vehicular Technology*, vol. 74, no. 7, pp. 11 546–11 551, 2025.
- [12] W. Guo, W. Zhang, P. Mu, and F. Gao, "High-Mobility OFDM Downlink Transmission With Large-Scale Antenna Array," *IEEE Transactions on Vehicular Technology*, vol. 66, no. 9, pp. 8600–8604, 2017.
- [13] Y. Hong, T. Thaj, and E. Viterbo, *Delay-Doppler Communications: Principles and Applications*. Netherlands: Elsevier, 2022, publisher Copyright: © 2022 Elsevier Inc. All rights reserved.
- [14] M. F. Keskin, H. Wymeersch, and V. Koivunen, "MIMO-OFDM Joint Radar-Communications: Is ICI Friend or Foe?" *IEEE Journal of Selected Topics in Signal Processing*, vol. 15, no. 6, pp. 1393–1408, 2021.
- [15] M. F. Keskin, C. Marcus, O. Eriksson, A. Alvarado, J. Widmer, and H. Wymeersch, "Integrated Sensing and Communications With MIMO-OTFS: ISI/ICI Exploitation and Delay-Doppler Multiplexing," *IEEE Transactions on Wireless Communications*, vol. 23, no. 8, pp. 10 229–10 246, 2024.
- [16] S. M. Kay, *Fundamentals of Statistical Signal Processing: Estimation Theory*. Englewood Cliffs, NJ: PTR Prentice-Hall, 1993.